Journal of Human Genetics (2015) 60, 53–61
© 2015 The Japan Society of Human Genetics All rights reserved 1434-5161/15
www.nature.com/jhg

ORIGINAL ARTICLE

Downregulation of the *microRNA-1/133a* cluster enhances cancer cell migration and invasion in lung-squamous cell carcinoma via regulation of *Coronin1C*

Hiroko Mataki[1], Hideki Enokida[2], Takeshi Chiyomaru[2], Keiko Mizuno[1], Ryosuke Matsushita[2], Yusuke Goto[3], Rika Nishikawa[3], Ikkou Higashimoto[1], Takuya Samukawa[1], Masayuki Nakagawa[2], Hiromasa Inoue[1] and Naohiko Seki[3]

Lung cancer is clearly the primary cause of cancer-related deaths worldwide. Recent molecular-targeted strategy has contributed to improvement of the curative effect of adenocarcinoma of the lung. However, such current treatment has not been developed for squamous cell carcinoma (SCC) of the disease. The new genome-wide RNA analysis of lung-SCC may provide new avenues for research and the development of the disease. Our recent microRNA (miRNA) expression signatures of lung-SCC revealed that clustered miRNAs miR-1/133a were significantly reduced in cancer tissues. Here, we found that restoration of both mature *miR-1* and *miR-133a* significantly inhibited cancer cell proliferation, migration and invasion. *Coronin-1C* (*CORO1C*) was a common target gene of the *miR-1/133a* cluster, as shown by the genome-wide gene expression analysis and the luciferase reporter assay. Silencing of *CORO1C* gene expression inhibited cancer cell proliferation, migration and invasion. Furthermore, *CORO1C*-regulated molecular pathways were categorized by using si-*CORO1C* transfectants. Further analysis of novel cancer signaling pathways modulated by the tumor-suppressive cluster *miR-1/133a* will provide insights into the molecular mechanisms of lung-SCC oncogenesis and metastasis.
Journal of Human Genetics (2015) **60,** 53–61; doi:10.1038/jhg.2014.111; published online 18 December 2014

INTRODUCTION

Lung cancer remains the most frequent cause of cancer-related death in developed countries.[1] Approximately 80% of lung cancers are classified histopathologically as non-small cell lung cancers. Patients with non-small cell lung cancers in advanced stages rarely survive more than 5 years despite aggressive chemotherapy, molecularly targeted therapy or chemoradiotherapy.[2] Non-small cell lung cancer is subdivided into four major histological subtypes with distinct pathological characteristics: adenocarcinoma, squamous cell carcinoma (SCC), large cell carcinoma and neuroendocrine cancer.[3] Molecular therapies such as gefitinib and erlotinib, which are specific for mutations in the epidermal growth factor receptor (*EGFR*; also known as *ERBB1*) gene and crizotinib, which is targeted against the *EML4-ALK* fusion gene, have been developed only for adenocarcinoma, but not for SCC in lung cancer (lung-SCC).[4–6] For patients with lung-SCC, the standard therapeutic approach remains to be chemotherapy. Therefore, there is a need for additional treatment options based on current RNA network analysis of lung-SCC.

The discovery of non-coding RNAs in the human genome was an important conceptual breakthrough in the post-genome sequencing era.[7] Improved understanding of non-coding RNAs is necessary for continued progress in cancer research. MicroRNAs (miRNAs) repress gene expression by inhibiting mRNA translation or by promoting mRNA degradation. Aberrant expression of miRNAs can contribute to cancer development, metastasis and drug resistance.[8–10] Currently, 2588 human mature miRNAs are registered at miRBase release 20.0 (http://microrna.sanger.ac.uk/). miRNAs are unique in their ability to regulate multiple protein-coding genes. Bioinformatic predictions indicate that miRNAs regulate ~30–60% of the protein-coding genes in the human genome.[11,12]

Our miRNA expression signatures of human cancers, including lung-SCC, revealed that expression of the *miR-1/133a* cluster is significantly reduced in several types of cancer tissues. Based on the signatures, we sequentially identified novel *miR-1/133a* cluster-regulated cancer pathways in prostate cancer, head and neck cancer, and urothelial carcinoma.[13–15] However, the functional role and molecular targets of the *miR-1/133a* cluster in lung-SCC is unclear. The aim of the present study was to investigate the functional significance of the *miR-1/133a* cluster and to identify the molecular targets regulated by these clustered miRNAs in lung-SCC cells.

[1]Department of Pulmonary Medicine, Graduate School of Medical and Dental Sciences, Kagoshima University, Kagoshima, Japan; [2]Department of Urology, Graduate School of Medical and Dental Sciences, Kagoshima University, Kagoshima, Japan and [3]Department of Functional Genomics, Graduate School of Medicine, Chiba University, Chiba, Japan
Correspondence: Dr N Seki, Department of Functional Genomics, Graduate School of Medicine, Chiba University, 1-8-1 Inohana Chuo-ku, Chiba 260-8670, Japan.
E-mail: naoseki@faculty.chiba-u.jp
Received 6 September 2014; revised 13 November 2014; accepted 13 November 2014; published online 18 December 2014

We found that restoration of either mature *miR-1* or *miR-133a* inhibited cancer cell proliferation, migration and invasion. Gene expression data and *in silico* database analysis showed that *coronin-1C* (*CORO1C*) was a potential target of *miR-1/133a* cluster regulation. The *CORO1C* gene encodes a member of the WD repeat protein family and is involved in a variety of cellular processes.[16,17] Down-regulating the *CORO1C* gene significantly inhibited cancer cell proliferation, migration and invasion. Furthermore, *CORO1C*-regulated molecular pathways were categorized by using si-*CORO1C* transfected cells. Further analysis of tumor-suppressive *miR-1/133a–CORO1C*-mediated cancer pathways might provides new insights into the potential mechanisms of lung-SCC oncogenesis and metastasis.

MATERIALS AND METHODS

Clinical specimens and RNA extraction

A total of 32 lung-SCCs and 22 normal lung specimens were collected from patients who underwent pneumonectomy at the Kagoshima University Hospital (Kagoshima, Japan) from 2010 to 2013. Archival formalin-fixed paraffin-embedded samples were used for quantitative real-time reverse transcription–PCR (qRT–PCR) analysis.

Samples were staged according to the International Association for the Study of Lung Cancer TNM classification and were histologically graded.[18] Our study was approved by the Institutional Review Board for Clinical Research of the Kagoshima University School of Medicine. Prior written informed consent and approval were provided by each patient.

Formalin-fixed paraffin-embedded tissues were sectioned to 10-μm thickness, and eight tissue sections were used for RNA extraction. Total RNA (including miRNA) was extracted using Recover All Total Nucleic Acid Isolation Kit (Ambion, Austin, TX, USA) according to the manufacturer's protocols. The integrity of the RNA was checked with the RNA 6000 Nano Assay Kit and a 2100 Bioanalyzer (Agilent Technologies, Santa Clara, CA, USA).

Cell culture

We used a human lung-SCC cell line (EBC-1) obtained from the Japanese Cancer Research Resources Bank (JCRB, Osaka, Japan). Cells were grown in RPMI 1640 medium supplemented with 10% fetal bovine serum and maintained in a humidified incubator (5% CO_2) at 37 °C.

Quantitative real-time reverse transcription–PCR

The procedure for PCR quantification was previously described.[13,19,20] TaqMan probes and primers were assay-on-demand gene expression products: *CORO1C* (assay ID: Hs00902568_m1, Applied Biosystems, Foster City, CA, USA), synaptotagmin-1 as an integral membrane proteins of synaptic vesicles (*SYT1*) (assay ID: Hs00194572_m1, Applied Biosystems), *STC2* (assay ID: Hs01063215_m1, Applied Biosystems) and cathepsin V as a group of lysosomal protease (*CTSV*) (assay ID: Hs00952036_m1, Applied Biosystems). Stem-loop RT–PCR for *miR-1* (assay ID: 002222, Applied Biosystems) and *miR-133a* (assay ID: 002246, Applied Biosystems) was used to quantify the expression levels of miRNAs according to the manufacturer's protocol. To normalize the data for quantification of mRNA and miRNAs, we used human *GUSB* (assay ID: Hs99999908_m1; Applied Biosystems) and *RNU48* (assay ID: 001006; Applied Biosystems), and the delta–delta Ct method was employed to calculate the fold change.

Transfection of EBC-1 cells with mature miRNA and small interfering RNA (siRNA)

The following mature miRNA species and siRNA species were used in the present study: Pre-miR miRNA precursors (P/N: AM 17100; Applied Biosystems), negative-control miRNA (P/N: AM 17111; Applied), Stealth Select RNAi siRNA, si-*CORO1C* (cat no. HSS119044, cat no. HS119045; Invitrogen, Carlsbad, CA, USA) and negative-control siRNA (D-001810-10; Thermo Fisher Scientific, Waltham, MA, USA). RNAs were incubated with Lipofectamine RNAiMAX reagent (Invitrogen) and OPTI-MEM (Invitrogen) as described previously.[13,19,20]

Treatment of EBC-1 cells with 5-azacitidine (an inhibitor of DNA methyltransferase) or trichostatin A (a histone deacetylase inhibitor)

Cells were treated with 5 μM of 5-azacitidine or 300 nM of trichostatin A. After 96 or 24 h of treatment, total RNA was extracted and subjected to qRT–PCR.

Cell proliferation, migration and invasion assays

Cells were transfected with 10 nM miRNAs or siRNA by reverse transfection and plated in 96-well plates at 8×10^3 cells per well. After 72 h, cell proliferation was determined with the XTT assay using a Cell Proliferation Kit II (Roche Molecular Biochemicals, Mannheim, Germany) as described previously.[13,19,20]

Cell migration activity was evaluated with wound healing assays. Cells were plated in six-well plates at 8×10^5 cells per well, and after 48 h of transfection the cell monolayer was scraped using a P-20 micropipette tip. The initial gap length (0 h) and the residual gap length 24 h after wounding were calculated from photomicrographs as described previously.[13,19,20]

Cell invasion assays were performed using modified Boyden chambers, consisting of transwell-precoated matrigel membrane filter inserts with eight micron pores in 24-well tissue culture plates (BD Biosciences, Bedford, MA, USA). RPMI 1640 medium containing 10% fetal bovine serum in the lower chamber served as the chemoattractant as described previously.[13,19,20] All experiments were performed in triplicate.

Identification of putative target genes of *miR-1/miR-133a* and *CORO1C*

Genes regulated by *miR-1/miR-133a* were obtained from the TargetScan database (http://www.targetscan.org). To investigate the expression status of candidate *miR-1/miR-133a* target genes in lung-SCC clinical specimens, we examined gene expression profiles in the gene expression omnibus database (accession number: GSE11117). In addition, we performed gene expression analysis using *miR-1* or *miR-133a*-transfected EBC-1 cells and si-*CORO1C*-transfected EBC-1 cells in comparison with control-transfected cells. Oligo-microarray human 60Kv (Agilent Technologies) was used for gene expression studies. Microarray procedures and data mining methods were described in previous studies.[13,15,20]

To identify molecular pathways regulated by *CORO1C* in EBC-1 cells, gene expression data were categorized according to the Kyoto Encyclopedia of Genes and Genomes (KEGG) pathways using the GENECODIS program (http://genecodis.dacya.ucm.es). The strategy behind this analysis procedure was previously described.[14,20]

Western blot analysis

Cells were harvested after 72 h of transfection, protein lysates (100 μg) were separated by NuPAGE on 4–12% bis-tris gels (Invitrogen) and transferred to polyvinylidene fluoride membranes. Immunoblotting was done with diluted (1:1000) monoclonal anti-coronin 3 antibody (ab77203; Abcam, Cambridge, UK) and GAPDH antibody (MAB374; Chemicon, Temecula, CA, USA). The membrane was washed and then incubated with horse radish peroxide-linked anti-rabbit immunoglobulin-G antibody (#7074; Cell Signaling, Danvers, MA, USA). Specific complexes were visualized with an echochemiluminescence (ECL) detection system (GE Healthcare, Little Chalfont, UK) as described previously.[13,15,20]

Plasmid construction and dual-luciferase reporter assays

Partial wild-type sequences of the *CORO1C* 3′-untranslated region (UTR) or those with a mutated *miR-1* target site (positions 111–118, 147–154 of the *CORO1C* 3′-UTR) and *miR-133a* target site (positions 147–154 and 371–377 of the *CORO1C* 3′-UTR) were inserted between the *Xho*I and *Pme*I restriction sites in the 3′-UTR of the hRluc gene in the psiCHECK-2 vector (C8021; Promega, Madison, WI, USA).

The synthesized DNA was cloned into the psiCHECK-2 vector. EBC-1 cells were transfected with 50 ng of the vector and 10 nM *miR-1* or *miR-133a* using Lipofectamine 2000 (Invitrogen). The activities of firefly and renilla luciferases in cell lysates were determined with a dual-luciferase assay system

(E1960; Promega). Normalized data were calculated as the ratio of renilla/firefly luciferase activities.

Statistical analysis

Relationships between two or more variables and numerical values were analyzed using the Mann–Whitney *U*-test or Bonferroni-adjusted Mann–Whitney *U*-test. In comparison among three or four variables, a non-adjusted statistical level of significance of $P<0.05$ corresponds to a Bonferroni-adjusted level of $P<0.0167$ or $P<0.0125$, respectively. Expert StatView software, version 4 (SAS Institute, Cary, NC, USA), was used in these analyses.

RESULTS

Expression levels of *miR-1* and *miR-133a* in lung-SCC specimens and cell line

To validate our past miRNA signature of lung-SCC results, we evaluated the expression of *miR-1* and *miR-133a* in lung-SCC tissues ($n=32$) and normal lung tissues ($n=22$). The background of patients and clinicopathological characteristics are summarized in Table 1. Representative formalin-fixed paraffin-embedded specimens that were used for RNA extraction and expression analysis in this study are shown in Supplementary Figure 1.

The expression levels of *miR-1* and *miR-133a* were significantly reduced in tumor tissues compared WITH corresponding non-cancerous tissues ($P<0.0001$; Figures 1a and b, respectively). Spearman's rank test showed a positive correlation between the expression of *miR-1* and that of *miR-133a* ($r=0.956$ and $P<0.0001$, Figure 1c).

There was a significant relationship between the expression level of *miR-1* or *miR-133a* and venous invasion. However, there was no significant correlation with other clinicopathological parameters (stage, grade and infiltration). In lung-SCC cell line, EBC-1 cells also exhibited low expression levels of *miR-1* and *miR-133a* compared with normal lung tissues (Figures 1a and b).

Treatment with trichostatin A significantly increased *miR-1* and *miR-133a* expression levels in EBC-1 cells, whereas 5-azacitidine had no effect on their expression levels (Supplementary Figure 2).

Effects of restoring *miR-1* and *miR-133a* on cell proliferation, migration and invasion activities of EBC-1 cells

To examine the functional roles of *miR-1* and *miR-133a*, we performed gain-of-function studies using miRNA transfection into EBC-1 cells. XTT assays revealed significant inhibition of cell proliferation in EBC-1 cells transfected with *miR-1* and *miR-133a* in comparison with mock-transfected cells and control transfectants (both $P<0.0001$, Figure 1d).

Moreover, wound healing assays revealed significant inhibition of cell migration in EBC-1 cells transfected with *miR-1* and *miR-133a* (both $P<0.0001$, Figure 1e, Supplementary Figure 3a). Similarly, matrigel invasion assays revealed that transfection with *miR-1* and *miR-133a* reduced cell invasion. Indeed, the number of invading cells was significantly decreased in EBC-1 cells transfected with *miR-1* and *miR-133a* (both $P<0.001$, Figure 1f, Supplementary Figure 3b).

It is plausible the *miR-1/133a* clusters may have important roles as tumor suppressors by targeting several oncogenic genes. However, we found no simultaneous effect of cell viability inhibition by *miR-1* and *miR-133a* co-transfection on EBC-1 cells (data not shown). A similar phenomenon has been shown in our previous articles on *miR-1/133a* and *miR-143/145* clusters in prostate cancer.[13,21]

Identification of candidate genes targeted by the *miR-1/133a* cluster

The TargetScan database indicated that a total of 3117 and 2216 genes were putative targets of *miR-1* and *miR-133a*, respectively. Moreover, 697 genes were common targets of both *miR-1* and *miR-133a*. Among the 697 common genes, 12 genes were upregulated in lung-SCC clinical specimens according to the gene expression omnibus database (accession number GSE11117). When we examined all the putative target sites of *miR-1* and *miR-133a*, four genes (*STC2, SYT1, CTSV* and *CORO1C*) had three conserved sites in total within their 3′-UTRs (Table 2). To gain further insight on which genes were affected by *miR-1* and *miR-133a* transfection, we performed microarray analysis of *miR-1* and *miR-133a* transfectants (EBC-1). Among the four genes,

Table 1 Characteristic of patients

(a)	n *(%)*
Lung cancer	
Total number	32
Median age (range)	71 (50–88)
Gender	
Male	30 (93.8)
Female	2 (6.2)
Pathological tumor stage	
IA	5 (15.6)
IB	7 (21.9)
IIA	4 (12.5)
IIB	5 (15.6)
IIIA	8 (25.0)
IIIB	1 (3.1)
Unkown	2 (6.3)
Differentiation	
Well	8 (25.0)
Moderately	19 (59.4)
Poorly	3 (9.4)
Unknown	2 (6.3)
Pleural invasion	
(+)	15 (46.9)
(−)	17 (53.1)
Venous invasion	
(+)	16 (50.0)
(−)	16 (50.0)
Lymphatic invasion	
(+)	16 (50.0)
(−)	16 (50.0)
Recurrence	
(+)	9 (28.1)
(−)	20 (62.5)
Unknown	3 (9.4)
(b)	n
Nomal lung	
Total number	22
Median age (range)	71 (50–88)
Gender	
Male	22
Female	0

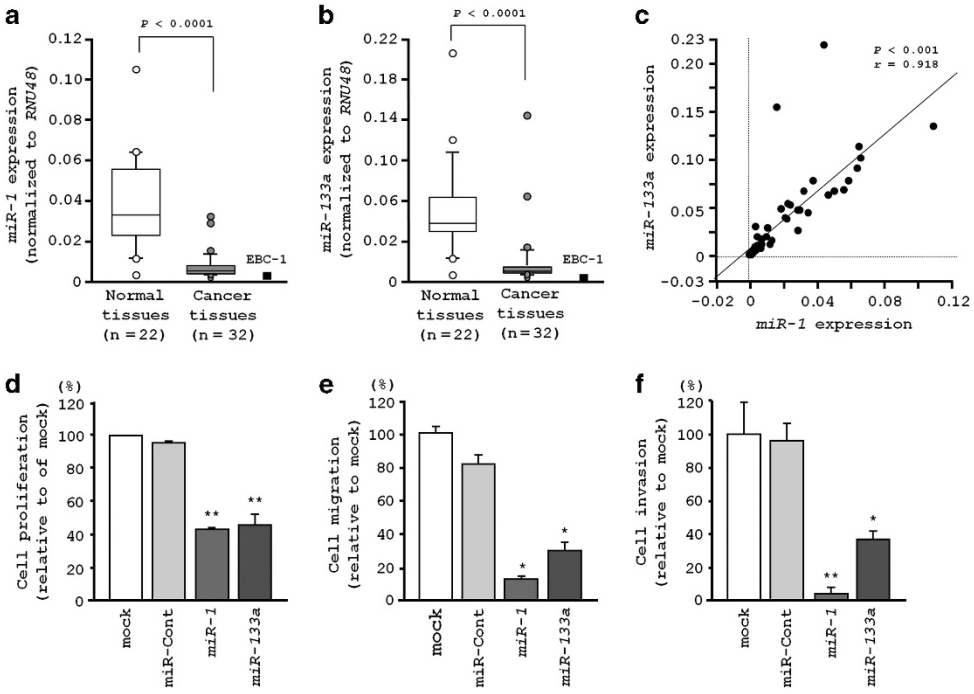

Figure 1 The expression levels of microRNA-1 (*miR-1*) and *miR-133a* in lung-squamous cell carcinoma (lung-SCC) clinical specimens and EBC-1 cells, and effects of restoring the miRNAs on cell viabilities. (**a**, **b**) The expression levels of *miR-1* (**a**) and *miR-133a* (**b**) in clinical specimens (lung-SCC and normal lung) and a lung-SCC cell line (EBC-1) were measured by quantitative real-time reverse transcription–PCR. *RNU48* was used as an internal control. Significances were determined by Mann–Whitney *U*-test. (**c**) Spearman's rank test showed a positive correlation between the expression of *miR-1* and that of *miR-133a* ($r=0.956$ and $P<0.0001$). (**d**) Cell proliferation was determined with XTT assays 72 h after transfection with 10 nM of *miR-1* or *miR-133a*. $^{**}P<0.0001$ (Bonferroni-adjusted Mann–Whitney *U*-test). (**e**) Cell migration activity was determined by migration assay 48 h after transfection. $^{**}P<0.0001$ (Bonferroni). (**f**) Cell invasion activity was determined by matrigel invasion assay 48 h after transfection. $^{**}P<0.0001$, $^{*}P=0.0004$ (Bonferroni).

Table 2 Common target genes of *miR-1* and *miR-133a* highly expressed in lung-SCC

									Expression (log_2 ratio)	
Entrez gene ID	*Gene symbol*	*Gene name*	*Log_2 ratio*	P-*value*	*miR-1 conserved site*	*miR-1 poorly conserved site*	*miR-133a conserved site*	*miR-133a poorly conserved site*	*EBC-1 miR-1 transfectants*	*EBC-1 miR-133a transfectants*
1830	*DSG3*	Desmoglein 3	6.52	0.005807	—	1	—	1	Not detected	Not detected
8614	*STC2*	Stanniocalcin 2	3.92	0.005807	1	1	—	1	0.57	0.17
1515	*CTSV*	Cathepsin V	3.22	0.005807	—	1	—	2	−0.94	−2.76
10397	*NDRG1*	N-myc downstream regulated 1	3.04	0.016289	—	1	1	—	−0.22	−1.39
6857	*SYT1*	Synaptotagmin I	2.33	0.029130	2	—	1	—	Not detected	0.46
23603	*CORO1C*	Coronin, actin-binding protein, 1C	2.23	0.023353	2	—	1	—	−2.55	−1.61
4288	*MKI67*	Marker of proliferation Ki-67	2.10	0.018385	—	1	—	1	−0.27	−0.47
51263	*MRPL30*	Mitochondrial ribosomal protein L30	1.89	0.017744	—	1	—	1	0.20	−0.26
6382	*SDC1*	Syndecan 1	1.69	0.019486	—	1	—	1	−2.30	−0.82
8087	*FXR1*	Fragile X mental retardation, autosomal homolog 1	1.62	0.019486	—	1	—	1	−0.90	−0.85
29979	*UBQLN1*	Ubiquilin 1	1.35	0.019486	—	1	—	1	−0.53	−1.79
3964	*LGALS8*	Lectin, galactoside-binding, soluble, 8	1.08	0.018385	—	1	1	—	0.67	0.73

Abbreviations: miR, microRNA; SCC, squamous cell carcinoma.

CORO1C was the most downregulated gene ($\log_2$ ratio < -1.5 in both *miR-1* and *miR-133a* transfectants) (Table 2). Therefore, we focused on *CORO1C* for further studies.

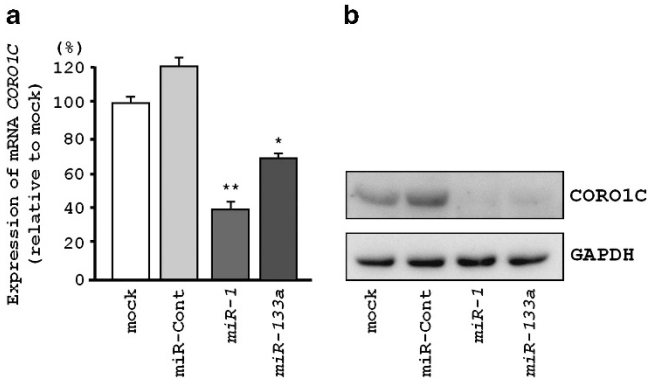

Figure 2 Direct regulation of CORO1C by microRNA-1 (*miR-1*) and *miR-133a* in EBC-1 cells. (**a**) *CORO1C* messenger RNA (mRNA) expression was evaluated by quantitative real-time reverse transcription–PCR 72 h after transfection with *miR-1* or *miR-133a*. *GUSB* was used as an internal control. $^{**}P<0.0001$, $^{*}P=0.0002$ (Bonferroni). (**b**) CORO1C protein expression was evaluated by Western blotting 72 h after transfection with *miR-1* or *miR-133a*. GAPDH was used as a loading control.

CORO1C was a direct target of the *miR-1/133a* cluster in EBC-1 cells

We performed qRT–PCR and Western blotting to confirm *CORO1C* gene and CORO1C protein downregulation by restoration of *miR-1* or *miR-133a* in EBC-1. The messenger RNA (mRNA) and protein expression levels of the *CORO1C* gene and its protein were significantly repressed in *miR-1 and miR-133a* transfectants in comparison with mock or miR-control transfectants (both $P<0.001$, Figure 2).

We then performed luciferase reporter assays in EBC-1 cells to determine whether *CORO1C* was directly regulated by *miR-1* and *miR-133a*. The TargetScan database predicted that there were two binding sites for *miR-1* in the 3′-UTR of *CORO1C* (positions 111–118 and 147–154; Figure 3a), and one binding site for *miR-133a* in the 3′-UTR of *CORO1C* (positions 371–377; Figure 3b). We used vectors encoding the partial wild-type sequence of the 3′-UTR of *CORO1C* mRNA, including the predicted *miR-1* or *miR-133a* target sites. We found that the luminescence intensity was significantly reduced by co-transfection with *miR-1* or *miR-133a* and the vector carrying the wild-type 3′-UTR of *CORO1C*, whereas transfection with the mutant vector (positions 111–118, 147–154 or 371–377 had been changed) blocked the decrease in luminescence ($P<0.0001$, Figures 3a and b). These data suggested that *miR-1* and *miR-133a* bound directly to specific sites in the 3′-UTR of *CORO1C* mRNA.

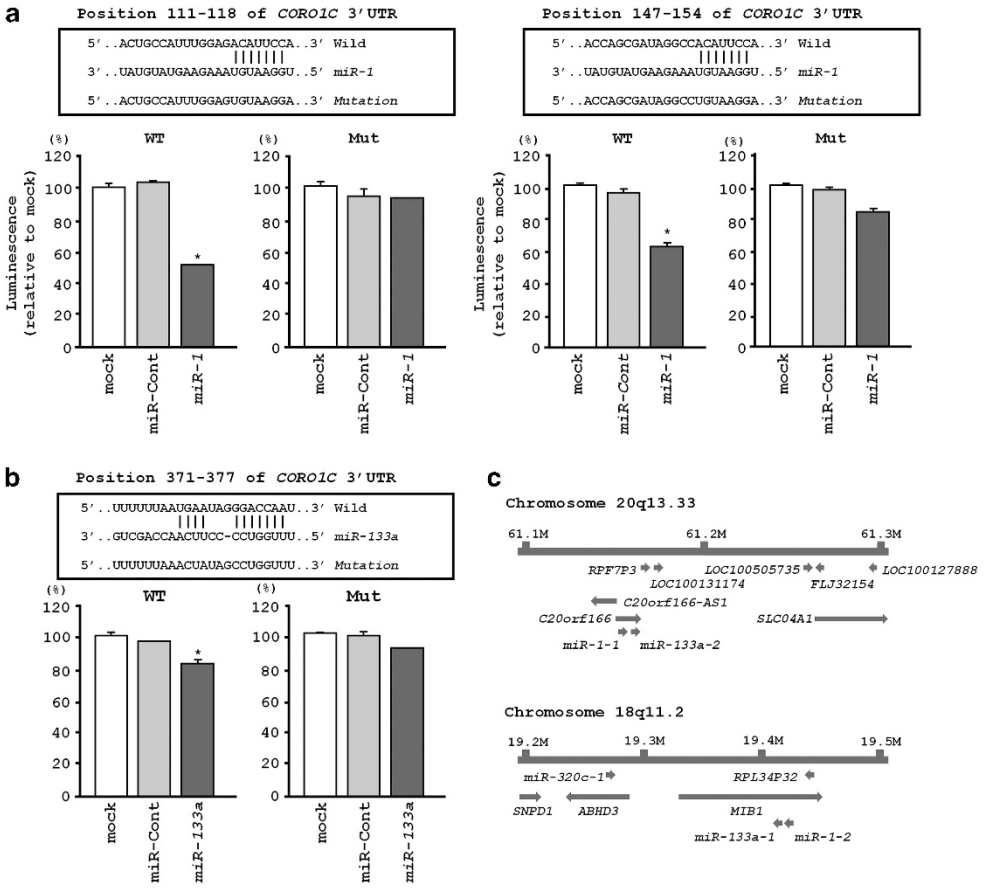

Figure 3 MicroRNA-1 (*miR-1*) and *miR-133a* binding sites in the 3′-untranslated region (3′-UTR) of *CORO1C*. (**a**, **b**) Luciferase reporter assays using vectors encoding putative *miR-1* and *miR-133a* target sites at positions 111–118, 147–154 and 371–377 for both wild type and mutants. *Renilla* luciferase values were normalized to firefly luciferase values. $^{*}P<0.0001$ (Bonferroni). (**c**) The clusters *miR-1-1/miR-133a-2* and *miR-1-2/miR-133a-1* are located in two different chromosomal regions 20q13.33 and 18q11.2, respectively.

Downregulation of *CORO1C* expression in EBC-1 cells affected proliferation, migration and invasion activities

To investigate the functional role of *CORO1C*, we performed loss-of-function studies using si-*CORO1C* transfectants. First, we evaluated the knockdown efficiency of si-*CORO1C* transfection in EBC-1 cells. Western blotting and qRT–PCR indicated that si-*CORO1C* effectively downregulated CORO1C expression in EBC-1 cells ($P<0.0001$, Figures 4a and b).

XTT assays demonstrated that cell proliferation was significantly inhibited in *si-CORO1C* transfectants in comparison with mock or si-control transfectants in EBC-1 cells ($P<0.005$, Figure 4c). Moreover, wound healing assays revealed significant inhibition of cell migration in si-*CORO1C* transfectants in comparison with mock or si-control transfectants in EBC-1 cells ($P<0.0001$, Figure 4d, Supplementary Figure 5a). Similarly, matrigel invasion assays revealed that the number of invading cells was significantly decreased when EBC-1 cells were transfected with si-*CORO1C* ($P<0.0001$, Figure 4e, Supplementary Figure 5b).

Identification of molecular pathways regulated by *CORO1C* in EBC-1 cells

To investigate the molecular pathways regulated by *CORO1C*, a genome-wide gene expression analysis was performed in EBC-1 cells transfected with si-*CORO1C*. A total of 967 genes were identified as being downregulated in si-*CORO1C* transfected cells compared with the control ($\log_2$ ratio < -0.2). We categorized the downregulated genes according to KEGG pathways, and a total of 29 pathways were identified as significantly enriched (Table 3). Among these pathways, we focused on 'pathways in cancer', 'focal adhesion', 'tight junction' and 'regulation of actin cytoskeleton' pathways because si-*CORO1C* significantly inhibited cancer cell migration and invasion. Genes involved in these pathways are listed in Supplementary Table 1.

DISCUSSION

Accumulating evidence has suggested that aberrantly expressed miRNAs disrupt tightly regulated RNA networks in cancer cells. These events are believed to initiate cancer cell development and metastasis.[8,9] Therefore, identification of differentially expressed miRNAs in cancer cells is the first step to elucidating novel miRNA-regulated molecular mechanisms in cancer cells. Expression signatures of various types of cancer tissues are important sources for the study of miRNAs in cancer. Based on these points, our group has determined the miRNA expression signatures in various cancers and thereby identified tumor-suppressive miRNAs.[15,22,23]

Recent genome-wide miRNA expression technologies have clarified that *miR-1/133a* and *miR-206/133b* clusters are to be altered in several types of human cancers.[24] In this study, we focused on *miR-1/133a*-clustered miRNAs because these miRNAs were frequently downregulated in various types of cancers, including lung-SCC.[24,25] Our present study showed that *miR-1* and *miR-133a* were significantly

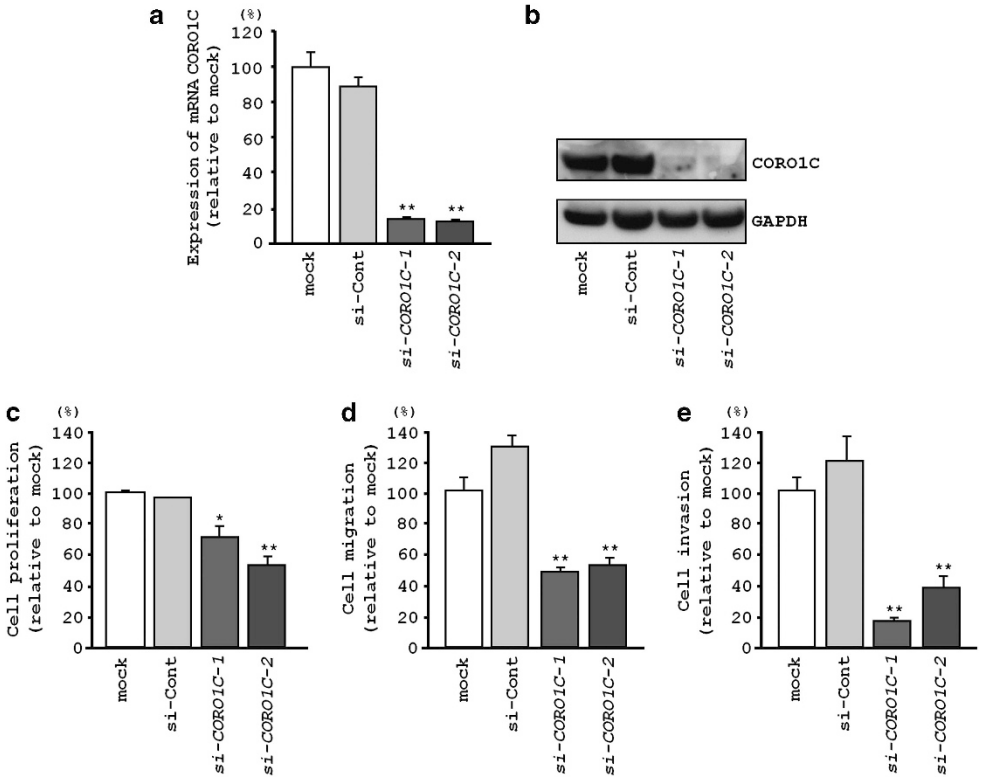

Figure 4 Silencing of CORO1C messenger RNA (mRNA) and protein expression by si-*CORO1C* transfection and effects of silencing of CORO1C on EBC-1 cell activities. (**a**) *CORO1C* mRNA expression was evaluated by quantitative real-time reverse transcription–PCR 72 h after transfection with *miR-1* or *miR-133a*. *GUSB* was used as an internal control. $^{**}P<0.0001$ (Bonferroni). (**b**) CORO1C protein expression was evaluated by Western blotting 72 h after transfection. GAPDH was used as a loading control. (**c**) EBC-1 cell proliferation was determined with XTT assays. $^{**}P<0.0001$, $^{*}P=0.0025$ (Bonferroni). (**d**) EBC-1 cell migration activity was determined by migration assay. $^{**}P<0.0001$ (Bonferroni). (**e**) EBC-1 cell invasion activity was determined by matrigel invasion assay. $^{**}P<0.0001$ (Bonferroni).

Table 3 Significantly enriched KEGG pathways regulated by si-*CORO1C* in lung-SCC cell

Number of genes	P-*value*		*Annotations*
23	0.000128	(KEGG) 05200	Pathways in cancer
23	1.11E-12	(KEGG) 03040	Spliceosome
19	0.000016	(KEGG) 04510	Focal adhesion
19	0.000001	(KEGG) 04141	Protein processing in endoplasmic reticulum
17	0.002517	(KEGG) 04010	MAPK signaling pathway
14	0.000299	(KEGG) 03013	RNA transport
14	0.000124	(KEGG) 04530	Tight junction
13	0.008132	(KEGG) 04144	Endocytosis
13	0.014305	(KEGG) 04810	Regulation of actin cytoskeleton
12	0.000772	(KEGG) 04110	Cell cycle
12	0.000422	(KEGG) 04670	Leukocyte transendothelial migration
10	0.000838	(KEGG) 05322	Systemic lupus erythematosus
9	0.032729	(KEGG) 04910	Insulin signaling pathway
9	0.002537	(KEGG) 03010	Ribosome
9	0.000958	(KEGG) 03008	Ribosome biogenesis in eukaryotes
8	0.000673	(KEGG) 04150	mTOR signaling pathway
8	0.002633	(KEGG) 04115	p53 signaling pathway
8	0.002564	(KEGG) 03018	RNA degradation
8	0.008958	(KEGG) 05222	Small cell lung cancer
7	0.004546	(KEGG) 05221	Acute myeloid leukemia
7	0.014504	(KEGG) 04520	Adherens junction
7	0.015441	(KEGG) 05412	Arrhythmogenic right ventricular cardiomyopathy
7	0.045052	(KEGG) 00240	Pyrimidine metabolism
6	0.017754	(KEGG) 04612	Antigen processing and presentation
6	0.027366	(KEGG) 05210	Colorectal cancer
6	0.044317	(KEGG) 05212	Pancreatic cancer
6	0.028469	(KEGG) 05416	Viral myocarditis
5	0.025143	(KEGG) 05219	Bladder cancer
5	0.046317	(KEGG) 00983	Drug metabolism—other enzymes

Abbreviations: KEGG, Kyoto encyclopedia of genes and genomes; MAPK, mitogen-activated protein kinase; miR, microRNA; mTOR, mammalian target of rapamycin; SCC, squamous cell carcinoma.

reduced in lung-SCC tissues and that they function as tumor suppressors by modulating cancer cell migration and invasion in lung-SCC. Our studies and other reports strongly suggest that the *miR-1/133a*-clustered miRNAs might act as tumor suppressors in various human cancers.[13–15,26]

The chromosomal location of the *miR-1/133a* cluster in the human genome is of significant interest. The *miR-1-1/miR-133a-2*, the *miR-1-2/miR-133a-1* and the *miR-206/miR-133b* clusters are located in three different chromosomal regions, that is, 20q13.33, 18q11.2 and 6p12.1, respectively. The mature sequence of *miR-1* differs from that of *miR-206* by four nucleotides.[24] The mature sequences of miR-*133a-1* and *miR-133a-2* possess identical sequences. The *miR-133b* sequence differs from *miR-133a* by a single nucleotide at the 3′-end.[24] Silencing epigenetic mechanisms of these clustered miRNAs have been investigated, DNA methylation-mediated *miR-1* downregulation was suggested in hepatocellular carcinoma and colorectal cancer.[27,28] In lung cancer cells, previous study and our data (Supplementary Figure 2) indicated that *miR-1* and *miR-133a* silencing might be caused by hypoacetylation of histones.[29] Detailed analyses will be necessary about epigenetic mechanism of *miR-1/133a* cluster in lung-SCC cells in future.

We also investigated the expression levels of *miR-206/133b* cluster in lung-SCC specimens. Our data indicated that these clustered miRNAs were downregulated in lung-SCC tissues compared with non-cancerous tissues (Supplementary Figure 6). Interestingly, our recent study showed that expression of mature *miR-206* also suppressed cancer cell proliferation, migration and invasion in lung-SCC cells by targeting both mRNA and protein levels of MET and EGFR (under submission).

The genes regulated by miRNA in cancer cells vary according to cancer types. Thus, identification of the targets regulated by the tumor-suppressive *miR-1/133a* cluster is important for clarifying our understanding of lung-SCC oncogenesis and metastasis. In this study, we identified common target genes of the *miR-1/133a* cluster using a combination of *in silico* analysis and gene expression analysis with *miR-1* and *miR-133a* transfectants. Using this strategy, we succeeded in proving that the tumor-suppressive *miR-1/133a* cluster-regulated oncogenic genes such as *TAGLN2* in bladder cancer, renal cell carcinoma and maxillary sinus SCC, and *PNP* in prostate cancer.[13–15] Moreover, we showed that restoration of *miR-133a* led to a reorganization of the actin cytoskeleton and a subsequent change in cell morphology, inhibitions of cell migration and invasion by direct targeting of actin-related protein 2/3 complex subunit 5 (*ARPC5*) in head and neck SCC.[30] Identification of these target genes might contribute to elucidation of novel cancer networks in lung-SCC.

In this study, we focused on the *CORO1C* gene. We evaluated the expression levels of four candidate genes (*STC2*, *SYT1*, *CTSV* and *CORO1C*) using miR-1 or miR-133a transfectants by qRT–PCR methods. Among them, three genes (*SYT1*, *CTSV* and *CORO1C*) were significantly downregulated by both restoration of *miR-1* and *miR-133a* in EBC-1 cell (Supplementary Figure 4). *CORO1C* is a member of coronin protein family, a WD-repeat-containing, actin-binding protein that regulates cell motility by coordination of actin filament turnover.[31,32] Other candidate genes, such as *SYT1* and *CTSV* were excluded in this study because they were well investigated in previous studies. Our present data clearly showed that *CORO1C* was directly regulated by both *miR-1* and *miR-133a* in lung-SCC cells. Furthermore, silencing of *CORO1C* gene expression significantly inhibited cancer cell migration and invasion. These results are consistent with past reports of gastric cancer and diffuse glioma.[33,34] According to the previous reports, silencing of *CORO1C* expression significantly inhibited cancer cell migration and invasion in human gastric and glioblastoma cell lines.[33,34] Furthermore, *CORO1C* was remarkably higher in tissues of lymph node metastases than primary gastric cancer tissues, and overexpression of *CORO1C* was associated with tumor-grade and lymph node metastasis.[33] More recently, it was reported that *miR-206* repressed cancer cell migration through direct regulation of *CORO1C* in triple-negative breast cancer cells.[35] These results indicated that downregulation of *miR-1/133a* cluster or

miR-206/133b cluster in cancer cells elevated the expression level of *CORO1C*, and these events might promote cancer cell migration and invasion.

For decades, the molecular mechanisms of cancer cell metastasis involving the regulation of the actin cytoskeleton have been intensively studied. Expression of CORO1C is localized at the leading edge of lamellipodia and invadopodia, and it physically interacts with the Arp2/3 complex.[31,32,36,37] Lamellipodia are thin, sheet-like membrane protrusions found at the leading edge of motile cells, and they are regulated by the Arp2/3 complex and cofilin.[37–39] Invadopodia are actin-rich membrane protrusions that are formed by invasive cells, involving several proteins such as the Arp2/3 complex, WASP, cofilin and coronins.[37–39] These results suggest that regulation of *CORO1C* by the *miR-1/133a* cluster might be an important mechanism for cancer cell migration and invasion.

To approach further functional roles of *CORO1C*, we performed genome-wide gene expression analysis using si-*CORO1C*-transfected EBC-1 cells to investigate *CORO1C*-regulated molecular pathways and targets. Several pathways that significantly contributed to cell migration and invasion were enriched downstream from *CORO1C*, such as 'pathway in cancer', 'focal adhesion', 'tight junction' and 'regulation of actin cytoskeleton' pathways. Several genes involved in these pathways were downregulated by both *si-CORO1C* and *miR-1/133a* transfectants, suggesting that these genes are involved in tumor-suppressive *miR-1/133a-CORO1C* pathway in lung-SCC cells. For example in 'pathways in cancer', several well-known oncogenes, such as *BIRC5*, *HIF1A*, *MYC*, *RUNX1*, VEGFC and *VEGFA*, might be involved in this network in lung-SCC cells (Supplementary Table 1). To better understand oncogenesis and metastasis in lung-SCC, it will be important to analyze genes involved in these pathways and their relationship with the *miR-1/133a-CORO1C*-mediated signal transduction.

In conclusion, *miR-1/133a*-clustered miRNAs were significantly downregulated in clinical lung-SCC specimens, and appeared to function as tumor suppressors through regulation of oncogenic *CORO1C*. Molecular pathways regulated by the tumor-suppressive *miR-1/133a* cluster might control actin cytoskeleton networks in cancer cells. Elucidation of oncogenic *CORO1C* pathways targeted by the tumor-suppressive *miR-1/133a* cluster may reveal novel effective therapeutic strategies for the treatment of lung-SCC.

CONFLICT OF INTEREST

The authors declare no conflict of interest.

1 Jemal, A., Bray, F., Center, M. M., Ferlay, J., Ward, E. & Forman, D. Global cancer statistics. *CA Cancer J. Clin.* **61**, 69–90 (2011).
2 Reck, M., Heigener, D. F., Mok, T., Soria, J. C. & Rabe, K. F. Management of non-small-cell lung cancer: recent developments. *Lancet.* **382**, 709–719 (2013).
3 Travis W. D. Pathology of lung cancer. *Clin. Chest Med.* **32**, 669–692 (2011)
4 Maemondo, M., Inoue, A., Kobayashi, K., Sugawara, S., Oizumi, S. & Isobe, H. *et al.* Gefitinib or chemotherapy for non-small-cell lung cancer with mutated EGFR. *N. Engl. J. Med.* **362**, 2380–2388 (2010).
5 Zhou, C., Wu, Y. L., Chen, G., Feng, J., Liu, X. Q. & Wang, C. *et al.* Erlotinib versus chemotherapy as first-line treatment for patients with advanced EGFR mutation-positive non-small-cell lung cancer (OPTIMAL, CTONG-0802): a multicentre, open-label, randomised, phase 3 study. *Lancet Oncol.* **12**, 735–742 (2011).
6 Shaw, A. T., Yeap, B. Y., Solomon, B. J., Riely, G. J., Gainor, J. & Engelman, J. A. *et al.* Effect of crizotinib on overall survival in patients with advanced non-small-cell lung cancer harbouring ALK gene rearrangement: a retrospective analysis. *Lancet Oncol.* **12**, 1004–1012 (2011).
7 Bartel, D. P. MicroRNAs: genomics, biogenesis, mechanism, and function. *Cell* **116**, 281–297 (2004).
8 Hobert, O. Gene regulation by transcription factors and microRNAs. *Science* **319**, 1785–1786 (2008).
9 Iorio, M. V. & Croce, C. M. MicroRNAs in cancer: small molecules with a huge impact. *J. Clin. Oncol.* **27**, 5848–5856 (2009).
10 Rolfo, C., Fanale, D., Hong, D. S., Tsimberidou, A. M., Piha-Paul, S. A. & Pauwels, P. *et al.* Impact of microRNAs in resistance to chemotherapy and novel targeted agents in non-small cell lung cancer. *Curr. Pharm. Biotechnol.* **15**, 475–485 (2014).
11 Filipowicz, W., Bhattacharyya, S. N. & Sonenberg, N. Mechanisms of post-transcriptional regulation by microRNAs: are the answers in sight? *Nat. Rev. Genet.* **9**, 102–114 (2008).
12 Friedman, J. M. & Jones, P. A. MicroRNAs: critical mediators of differentiation, development and disease. *Swiss Med. Wkly.* **139**, 466–472 (2009).
13 Kojima, S., Chiyomaru, T., Kawakami, K., Yoshino, H, Enokida, H. & Nohata, N. *et al.* Tumour suppressors miR-1 and miR-133a target the oncogenic function of purine nucleoside phosphorylase (PNP) in prostate cancer. *Br. J. Cancer* **106**, 405–413 (2012).
14 Nohata, N., Hanazawa, T., Kikkawa, N., Sakurai, D., Sasaki, K. & Chiyomaru, T. *et al.* Identification of novel molecular targets regulated by tumor suppressive miR-1/miR-133a in maxillary sinus squamous cell carcinoma. *Int. J. Oncol.* **39**, 1099–1107 (2011).
15 Yoshino, H., Chiyomaru, T., Enokida, H., Kawakami, K., Tatarano, S. & Nishiyama, K. *et al.* The tumour-suppressive function of miR-1 and miR-133a targeting TAGLN2 in bladder cancer. *Br. J. Cancer* **104**, 808–818 (2011).
16 Samarin, S. N., Koch, S., Ivanov, A. I., Parkos, C. A. & Nusrat, A. Coronin 1C negatively regulates cell-matrix adhesion and motility of intestinal epithelial cells. *Biochem. Biophys. Res. Commun.* **391**, 394–400 (2010).
17 Xavier, C. P., Rastetter, R. H., Stumpf, M., Rosentreter, A., Müller, R. & Reimann, J. *et al.* Structural and functional diversity of novel coronin 1C (CRN2) isoforms in muscle. *J. Mol. Biol.* **393**, 287–299 (2009).
18 Goldstraw, P., Crowley, J., Chansky, K., Giroux, D. J., Groome, P. A. & Rami-Porta, R. *et al.* The IASLC Lung Cancer Staging Project: proposals for the revision of the TNM stage groupings in the forthcoming (seventh) edition of the TNM Classification of malignant tumours. *J. Thorac. Oncol.* **2**, 706–714 (2007).
19 Kinoshita, T., Nohata, N., Hanazawa, T., Kikkawa, N., Yamamoto, N. & Yoshino, H. *et al.* Tumour-suppressive microRNA-29s inhibit cancer cell migration and invasion by targeting laminin-integrin signalling in head and neck squamous cell carcinoma. *Br. J. Cancer* **109**, 2636–2645 (2013).
20 Nohata, N., Hanazawa, T., Kinoshita, T., Inamine, A., Kikkawa, N. & Itesako, T. *et al.* Tumour-suppressive microRNA-874 contributes to cell proliferation through targeting of histone deacetylase 1 in head and neck squamous cell carcinoma. *Br. J. Cancer* **108**, 1648–1658 (2013).
21 Kojima, S., Enokida, H., Yoshino, H., Itesako, T., Chiyomaru, T. & Kinoshita, T. *et al.* The tumor-suppressive microRNA-143/145 cluster inhibites cell migration and invasion by targetingGOLM1 in prostate cancer. *J. Hum. Genet.* **59**, 78–87 (2014).
22 Itesako, T., Seki, N., Yoshino, H., Chiyomaru, T., Yamasaki, T. & Hidaka, H. *et al.* The microRNA expression signature of bladder cancer by deep sequencing: the functional significance of the miR-195/497 cluster. *PLoS ONE* **9**, e84311 (2014).
23 Hidaka, H., Seki, N., Yoshino, H., Yamasaki, T., Yamada, Y. & Nohata, N. *et al.* Tumor suppressive microRNA-1285 regulates novel molecular targets: aberrant expression and functional significance in renal cell carcinoma. *Oncotarget* **3**, 44–57 (2012).
24 Nohata, N., Hanazawa, T., Enokida, H. & Seki, N. microRNA-1/133a and microRNA--206/133b clusters: dysregulation and functional roles in human cancers. *Oncotarget* **3**, 9–21 (2012).
25 Moriya, Y., Nohata, N., Kinoshita, T., Mutallip, M., Okamoto, T. & Yoshida, S. *et al.* Tumor suppressive microRNA-133a regulates novel molecular networks in lung squamous cell carcinoma. *J. Hum. Genet.* **57**, 38–45 (2012).
26 Rao, P. K., Missiaglia, E., Shields, L., Hyde, G., Yuan, B. & Shepherd, C. J. *et al.* Distinct roles for miR-1 and miR-133a in the proliferation and differentiation of rhabdomyosarcoma cells. *FASEB J.* **24**, 3427–3437 (2010).
27 Datta, J., Kutay, H., Nasser, M. W., Nuovo, G. J., Wang, B. & Majumder, S. *et al.* Methylation mediated silencing of microRNA-1 geneand its role in hepatocellular carcinogenesis. *Cancer Res.* **68**, 5049–5058 (2008).
28 Suzuki, H., Takatsuka, S., Akashi, H., Yamamoto, E., Nojima, M. & Maruyama, R. *et al.* Genome-wide profiling of chromatin signatures reveals epigenetic regulation of microRNA genes in colorectal cancer. *Cancer Res.* **71**, 5646–5658 (2011).
29 Nasser, M. W., Datta, J., Nuovo, G., Kutay, H., Moiwala, T. & Majumder, S. *et al.* Down-regulation of micro-RNA-1 (miR-1) in lung cancer. Suppression of tumorigenic property of lung cancer cells and their sensitization to doxorubicin-induced apoptosis by miR-1. *J. Biol. Chem.* **283**, 33394–33405 (2008).
30 Kinoshita, T., Nohata, N., Watanabe-Takano, H., Yoshino, H., Hidaka, H. & Fujimura, L. *et al.* Actin-related protein 2/3 complex subunit 5 (ARPC5) contributes to cell migration and invasion and is directly regulated by tumor-suppressive microRNA-133a in head and neck squamous cell carcinoma. *Int. J. Oncol.* **40**, 1770–1778 (2012).
31 Rosentreter, A., Hofmann, A., Xavier, C. P., Stumpf, M., Noegel, A. A. & Clemen, C. S. Coronin 3 involvement in F-actin-dependent processes at the cell cortex. *Exp. Cell Res.* **313**, 878–895 (2007).
32 Spoerl, Z., Stumpf, M., Noegel, A. A. & Hasse, A. Oligomerization, F-actin interaction, and membrane association of the ubiquitous mammalian coronin 3 are mediated by its carboxyl terminus. *J. Biol. Chem.* **277**, 48858–48867 (2002).
33 Ren, G., Tian, Q., An, Y., Feng, B., Lu, Y. & Liang, J. *et al.* Coronin 3 promotes gastric cancer metastasis via the up-regulation of MMP-9 and cathepsin K. *Mol. Cancer* **11**, 67 (2012).

34 Thal, D., Xavier, C. P., Rosentreter, A., Linder, S., Friedrichs, B. & Waha, A. *et al.* Expression of coronin-3 (coronin-1C) in diffuse gliomas is related to malignancy. *J. Pathol.* **214**, 415–424 (2008).
35 Wang, J., Tsouko, E., Jonsson, P., Bergh, J., Hartman, J. & Aydogdu, E. *et al.* miR-206 inhibits cell migration through direct targeting of the actin-binding protein Coronin 1C in triple-negative breast cancer. *Mol. Oncol.* **8**, 1690–1702 (2014).
36 Chan, K. T., Creed, S. J. & Bear, J. E. Unraveling the enigma: progress towards understanding the coronin family of actin regulators. *Trends Cell Biol.* **21**, 481–488 (2011).
37 Ziemann, A., Hess, S., Bhuwania, R., Linder, S., Kloppenburg, P. & Noegel, A. A. *et al.* CRN2 enhances the invasiveness of glioblastoma cells. *Neuro Oncol* **15**, 548–561 (2013).
38 Carlier, M. F. & Pantaloni, D. Control of actin assembly dynamics in cell motility. *J. Biol. Chem.* **282**, 23005–23009 (2007).
39 Yamaguchi, H., Lorenz, M., Kempiak, S., Sarmiento, C., Coniglio, S. & Symons, M. *et al.* Molecular mechanisms of invadopodium formation: the role of the N-WASP-Arp2/3 complex pathway and cofilin. *J. Cell Biol.* **168**, 441–452 (2005).

Supplementary Information accompanies the paper on Journal of Human Genetics website (http://www.nature.com/jhg)